

Coordinate-Based Bundle Adjustment – Advanced Network Adjustment Model for Polar Measurement Systems

M. Lösler, C. Eschelbach, R. Haas

Abstract To fulfill the requirements on local-ties formulated by GGOS, high precision instruments and rigorous uncertainty propagation are necessary. To evaluate the results of e.g. high performance total stations or laser trackers, the accuracy-limiting parameters of the measurement process have to be quantified and projected onto an uncertainty model. Using the generally across disciplines accepted *Guide to the Expression of Uncertainty in Measurement* (GUM) a transparent and traceable stochastic model can be derived. A Cartesian coordinate-based bundle adjustment is suggested, to integrate the local measurements into a global context avoiding gravitational influences. The included comprehensive uncertainty model is based on a specific geometric model of a polar measurement system and takes instrument specific and target dependent error parameters into account.

Keywords Laser Tracker, Total Station, Guide to the Expression of Uncertainty in Measurement, Local Tie, Network Adjustment, Uncertainty

Michael Lösler, michael.loesler@fb1.fra-uas.de
Cornelia Eschelbach, cornelia.eschelbach@fb1.fra-uas.de
Frankfurt University of Applied Sciences, Laboratory for Industrial Metrology, Nibelungenplatz 1, DE-60318 Frankfurt am Main, Germany

Rüdiger Haas, rudiger.haas@chalmers.se
Chalmers University of Technology, Onsala Space Observatory SE-439 92 Onsala, Sweden

1 Introduction

An interdisciplinary collaboration requires standard notations and terminologies as well as the acceptance of analytical procedures. An analysis must be transparent and traceable. In the field of metrology, the *Guide to the Expression of Uncertainty in Measurement* (GUM) was introduced in 1995 and supplemented in 1999 (cf. GUM (2008a), GUM (2008b)). The GUM specifies two distinct types of uncertainty classes called type-A and type-B. Whereas uncertainties of type-A are based on methods of evaluation of uncertainty by statistical analysis of multiple readings of the same measurement, type-B uncertainties make use of non-statistical approaches. The application of statistical analysis like the method of least-squares or the usage of Monte-Carlo techniques is well known in geodesy and are counted among type-A uncertainties. In the easiest case, the result is given by the sample mean, and the corresponding type-A uncertainty is represented by the experimental standard deviation called standard uncertainty. Type-B uncertainties are evaluated by scientific knowledge or experiences about the measurement process, calibration reports or manufacturer specifications, and cannot be obtained from repeated measurements. The combined standard uncertainty that contains type-A as well as type-B uncertainties is derived by the propagation of uncertainties (cf. GUM (2008a)). Although modern instruments like GNSS antennas, total stations, laser scanners and high precision laser trackers provide the coordinates of an observed position at the push of a button, complex background processes and the amount of parameters influencing and limiting the accuracy have to be kept in mind.

The following sections describe several effects that restrict the accuracy of a polar measurement. By assigning the identified error parameters and their corresponding uncertainties to the measurement process, type-A as well as type-B uncertainties of an observed position can be estimated and introduced during the network adjustment.

2 Coordinate-based network adjustment

In classical geodesy, the observed polar observations are combined during a network adjustment to derive spatial coordinates and corresponding uncertainties. Depending on the extent of the local network and the accuracy requirements, the influence of the curvature of the earth cannot be neglected. To overcome the influence of the inclination, different analysis strategies are developed (e.g. Schwarz (1994), Awange and Grafarend (2005)).

2.1 Functional model

In metrology, the influence of the curvature of the earth is mostly disregarded, because instruments like coordinate measuring machines and laser trackers are unrelated to the gravity field. Fig. 1 depicts a local tie measurement at the Onsala Space Observatory with a laser tracker LTD840, which is not related to the gravity field. To combine several stations, coordinate-based algorithms are developed in metrology (e.g. Calkins (2002), Lösler and Eschelbach (2012)).



Fig. 1 Local Tie Measurement at Onsala Space Observatory with Leica Laser Tracker LTD840.

For this purpose, the polar observations of the i th point \mathbf{p} of the j th station are converted into Cartesian spatial coordinates

$$\mathbf{p}_{i,j}(\Theta, \Phi, d) = \begin{pmatrix} x \\ y \\ z \end{pmatrix}_{i,j} = \begin{pmatrix} d \sin \Phi \cos \Theta \\ d \sin \Phi \sin \Theta \\ d \cos \Phi \end{pmatrix}_{i,j}. \quad (1)$$

Here, the slope distance is denoted by d , and Θ and Φ are the yaw and pitch angle w.r.t. the local station coordinate system, respectively. The usage of Eq. 1 assumes a perfect instrument. Fig. 2 shows possible deviations from the ideal case, e.g. an axis-offset or misalignment of the distance measurement unit. Most of these

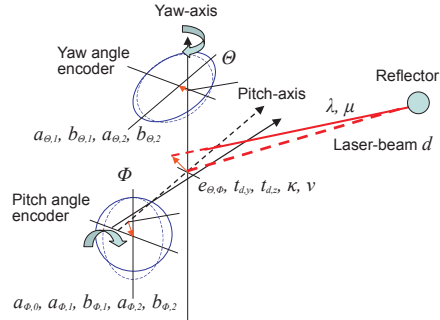


Fig. 2 Irregularities of a Polar Measurement Instrument (Hughes et al., 2011).

errors are compensated by the manufactures firmware and only a few errors can be rechecked by the instrument operator. Based on the work of Muralikrishnan (2009), a compensation model for mobile laser trackers is suggested by Hughes et al. (2011). The corrected slope distance \hat{d} results by adding the distance dependent scaling factor μ and the displacement offset λ .

$$\hat{d} = (1 + \mu)d + \lambda \quad (2)$$

The angle encoder errors are parameterized as Fourier series.

$$\hat{\Theta} = \Theta + \sum_{q=1}^{n_q} (a_{\Theta,q} \cos q\Theta + b_{\Theta,q} \sin q\Theta) \quad (3)$$

$$\hat{\Phi} = \Phi + a_{\Phi,0} + \sum_{q=1}^{n_q} (a_{\Phi,q} \cos q\Phi + b_{\Phi,q} \sin q\Phi) \quad (4)$$

where a_q and b_q represents the Fourier coefficients. The harmonic order of the Fourier series can be restricted to the order of $n_q = 2$ (Lewis et al., 2011).

The conversion of the polar observations into their Cartesian representation w.r.t. the irregularities of the observation instrument can be expressed by

$$\mathbf{p}_{i,j}(\hat{\Theta}, \hat{\Phi}, \hat{d}) = \mathbf{p}_0 + \mathbf{b}(\hat{\Theta}, \hat{\Phi}) + \hat{d}\mathbf{n}(\hat{\Theta}, \hat{\Phi}) \quad (5)$$

with

$$\mathbf{b}(\hat{\Theta}, \hat{\Phi}) = \mathbf{R}_{\hat{\Theta}}^z \begin{pmatrix} e_{\Theta, \Phi} \\ 0 \\ 0 \end{pmatrix} + \mathbf{R}_{\hat{\Theta}}^z \mathbf{R}_{\hat{\Phi}}^x \mathbf{R}_{\hat{\Phi}-\frac{\pi}{2}}^y \mathbf{R}_{-\kappa}^x \begin{pmatrix} t_{d,x} - e_{\Theta, \Phi} \\ t_{d,y} \\ t_{d,z} \end{pmatrix} \quad (6)$$

and

$$\mathbf{n}(\hat{\Theta}, \hat{\Phi}) = \mathbf{R}_{\hat{\Theta}}^z \mathbf{R}_{\hat{\Phi}}^x \mathbf{R}_{\hat{\Phi}-\frac{\pi}{2}}^y \mathbf{R}_{-\kappa}^x \mathbf{R}_{\hat{\nu}}^z \begin{pmatrix} 1 \\ 0 \\ 0 \end{pmatrix}. \quad (7)$$

The vector \mathbf{p}_0 summarizes the coordinates of the station and \mathbf{b} considers the axis-offset $e_{\Theta, \Phi}$ and the centering error of the distance measurement unit $t_d = (t_{d,x} \ t_{d,y} \ t_{d,z})^T$. The trunnion axis error κ and the horizontal collimation error ν are compensated by the vector \mathbf{n} . Even if the model was derived for laser trackers, it is also valid for total stations and laser scanners.

A conformal spatial seven-parameters transformation is used to combine the observed coordinates $\mathbf{p}_{i,j}$ of the j th station with the global coordinate system \mathbf{P}_i . The global datum can be defined as (local) topocentric coordinate system or as a global geocentric one like the ITRF.

$$\mathbf{p}_{i,j} = \mathbf{T}_j + m_j \mathbf{R}_j \mathbf{P}_i \quad (8)$$

Here, \mathbf{T} denotes the translation vector, m is the scaling parameter, which is applied uniformly to all axes, and \mathbf{R} represents the rotation matrix. A common Gauß-Markov model can be used (e.g. Mikhail and Ackerman (1976), Koch (1999)) to derive the global coordinates \mathbf{P}_i and the unknown transformation parameters of each station.

$$\mathbf{A}\mathbf{x} = \mathbf{l} + \mathbf{v} \quad (9)$$

The Jacobi matrix \mathbf{A} can be divided by column-sorting in a coordinate part \mathbf{A}_P and a part \mathbf{A}_T , which contains the transformation parameters of each station. The local coordinates of each station are given by the (reduced) observation vector \mathbf{l} , the vector \mathbf{v} contains the

observational errors, and the unknown parameters are denoted by $\mathbf{x} = (\mathbf{x}_P \ \mathbf{x}_{T,1} \ \mathbf{x}_{T,j} \ \mathbf{x}_{T,k})^T$.

$$\begin{pmatrix} A_{P,1} & A_{T,1} & 0 & 0 \\ A_{P,j} & 0 & A_{T,j} & 0 \\ A_{P,k} & 0 & 0 & A_{T,k} \end{pmatrix} \begin{pmatrix} x_P \\ x_{T,1} \\ x_{T,j} \\ x_{T,k} \end{pmatrix} = \begin{pmatrix} l_{p,1} \\ l_{p,j} \\ l_{p,k} \end{pmatrix} + \begin{pmatrix} v_{p,1} \\ v_{p,j} \\ v_{p,k} \end{pmatrix} \quad (10)$$

If available, prior results or additional GNSS observations \mathbf{x}_{GNSS} can be introduced to define the geodetic datum of the network.

$$\begin{pmatrix} \mathbf{A}_P & \mathbf{A}_T \\ \mathbf{E} & \mathbf{0} \end{pmatrix} \begin{pmatrix} \mathbf{x}_P \\ \mathbf{x}_T \end{pmatrix} = \begin{pmatrix} \mathbf{l}_P \\ \mathbf{l}_{GNSS} \end{pmatrix} + \begin{pmatrix} \mathbf{v}_P \\ \mathbf{v}_{GNSS} \end{pmatrix} \quad (11)$$

The stochastic model of this extended model reads

$$\begin{pmatrix} \mathbf{Q}_P & \mathbf{0} \\ \mathbf{0} & \mathbf{Q}_{GNSS} \end{pmatrix}. \quad (12)$$

To restrict the number of estimated transformation parameters, e.g. to fix the scale parameter to $m = 1$ or to rectify the defect of the normal equation matrix in case of a free network adjustment, additional restrictions $\mathbf{C}^T \mathbf{x} = \mathbf{c}$ can be applied (cf. Lösler and Eschelbach (2012))

$$\begin{pmatrix} \mathbf{N} & \mathbf{C} \\ \mathbf{C}^T & \mathbf{0} \end{pmatrix}^{-1} \begin{pmatrix} \mathbf{n} \\ \mathbf{c} \end{pmatrix} = \begin{pmatrix} \mathbf{x} \\ \mathbf{k} \end{pmatrix}, \quad (13)$$

where $\mathbf{N} = \mathbf{A}^T \mathbf{Q}_{ll}^{-1} \mathbf{A}$ and $\mathbf{n} = \mathbf{A}^T \mathbf{Q}_{ll}^{-1} \mathbf{l}$ are substitutions, and \mathbf{k} contains the Lagrange multipliers (e.g. Koch (1999)). With $\mathbf{Q}_{kk} = (\mathbf{C}^T \mathbf{N}^{-1} \mathbf{C})^{-1}$ the variance-covariance matrix \mathbf{Q}_{xx} of the unknown parameters \mathbf{x} are given by

$$\mathbf{Q}_{xx} = \mathbf{N}^{-1} - \mathbf{N}^{-1} \mathbf{C} \mathbf{Q}_{kk} \mathbf{C}^T \mathbf{N}^{-1} \quad (14)$$

2.2 Stochastic model

The stochastic model describes the a-prior uncertainties of the measurement process and allows for combining different types of observations w.r.t. their uncertainties. In general, the uncertainties are a composition of various parameters and distributions (e.g. GUM (2008a), GUM (2008b)).

The geometrically related parameters of the instrument shown in Eq. 5 are equivalent for all observations. In addition, each measurement can be considered as a realization of a random experiment. Therefore, a tar-

get centering error ζ , a resolution limiting error of the digital output ξ , and a random error τ should be introduced. Eqs. 2, 3 and 4 become

$$\hat{d} = (1 + \mu + \tau_d)d + \lambda + \zeta_d + \xi_d, \quad (15)$$

$$\hat{\Theta} = \Theta + \tau_\Theta + \xi_\Theta + \frac{\zeta_\Theta}{d}\rho + a_{\Theta,0} + \sum_{q=1}^{n_q} (a_{\Theta,q} \cos q\Theta + b_{\Theta,q} \sin q\Theta), \quad (16)$$

$$\hat{\Phi} = \Phi + \tau_\Phi + \xi_\Phi + \frac{\zeta_\Phi}{d}\rho + a_{\Phi,0} + \sum_{q=1}^{n_q} (a_{\Phi,q} \cos q\Phi + b_{\Phi,q} \sin q\Phi), \quad (17)$$

where $\rho = \frac{\pi}{200 \text{ gon}}$ denotes the angle conversion factor between radian and gon.

If forced centering or wooden tripods are used, the uncertainties of the station \mathbf{Q}_{p_0} have to be taken into account (Lösler and Eschelbach, 2012). The a-priori variance-covariance matrix \mathbf{Q}_p of statically observed coordinates \mathbf{p} results by substituting Eq. 15, 16 and 17 in Eq. 5 and applying the propagation of uncertainty.

2.3 Systematic effects

During a measurement process several effects limit the accuracy. Most of these effects are of random nature but there are also systematic effects that distort the results unilaterally. For example, the laser beam of the distance measurement unit is effected by meteorology and a non-representative survey of the meteorological parameters yields in systematic errors. Whereas this effect is well-known, the influence of misaligned glass body reflectors is not. To avoid systematic lateral $\epsilon_{\text{lateral}}$ and radial ϵ_{radial} errors, it is important to align the normal of the reflector surface to the line of sight (e.g. Pauli (1969), Rüeger (1990)). The magnitude of the errors caused by a misaligned reflector depends on the reflector type, size and on the angle of incidence δ .

$$\epsilon_{\text{radial}} = d \left(n_r - \sqrt{n_r^2 - \sin^2 \delta} \right) - e(1 - \cos \delta) \quad (18)$$

$$\epsilon_{\text{lateral}} = (d - e) \sin \delta - d \sec \delta_G \sin(\delta - \delta_G) \quad (19)$$

where $\delta_G = \arcsin \frac{\sin \delta}{n_r}$. The distance between the front surface of the prism and the center-symmetric point is denoted by e , while d is the distance between the front

surface of the prism and the corner point of the triple prism, and $n_r \approx 1.52$ represents the ratio of the group refractive indices of glass and air (Rüeger (1990)).

The systematic errors depend on the angle of incidence δ . Fig. 3 depicts the resulting systematic errors for various reflector sizes. Even if small size glass body reflectors yield in lower errors, these kind of reflectors reflect only a small part of the instrument's laser beam. Due to the small spot size, the likelihood for measurement failure is increased.

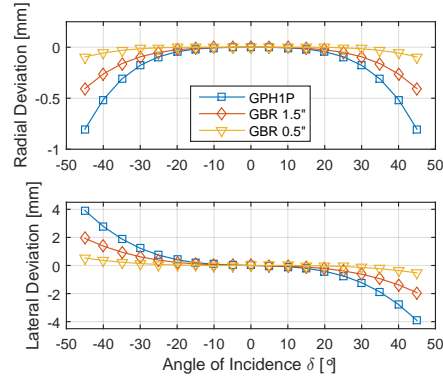


Fig. 3 Radial and Lateral Deviations caused by Reflector Misalignment for Precision Reflector GPH1P, Glass Ball Reflector 1.5'' and 0.5''.

During reference point determination, a misalignment of the reflectors is unavoidable, because of the rotation characteristic of the radio telescope. As shown by (Lösler et al., 2013) the systematic errors can be corrected for all radio telescope orientations. The remaining residual uncertainty is similar to the centering error ζ and can be taken into account in the network adjustment process (Lösler et al., 2015). Fig. 4 shows a comparison of corrected and uncorrected spatial positions.

3 Conclusion

A proper and traceable uncertainty budgeting is important in order to archive reliable results. An incomplete stochastic model or an unrepresentative sample of the population effects the estimated uncertainties (cf. Hennes (2007), Xu (2013)). In most cases the results are too optimistic and the derived confidence in-

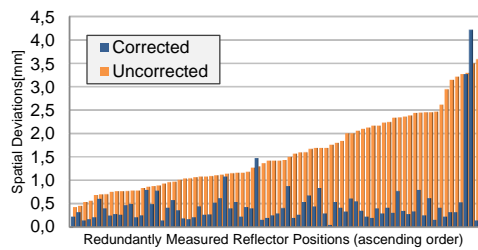


Fig. 4 Comparison of Corrected and Uncorrected Spatial Positions (Lösler et al., 2015).

tervals do not reflect the true uncertainties. By using common network adjustment tools, only a few uncertainties can be taken into account. Following the *Guide to the Expression of Uncertainty in Measurement* (GUM) a coordinate-based network adjustment is developed that includes a comprehensive uncertainty budgeting.

Moreover, the use of spatial similarity transformations paves a simple way to provide local observations in a global context like the ITRF. Whereas in conventional approaches the ITRF-transformation process is carried out as a final step, in our approach the transformation into the global reference frame takes place right in the beginning of the bundle adjustment.

References

- Awange JL, Grafarend EW (2005) *Solving Algebraic Computational Problems in Geodesy and Geoinformatics*, Springer, Heidelberg/Berlin.
- Calkins JM (2002) *Quantifying Coordinate Uncertainty Fields in Coupled Spatial Measurement systems*. Dissertationen, Faculty of the Virginia Polytechnic Institute and State University, Virginia.
- GUM (2008a) *Evaluation of measurement data – Guide to the expression of uncertainty in measurement*. JCGM 100:2008, GUM 1995 with minor corrections, <http://www.bipm.org/en/publications/guides/gum.html>, retrieved: 2015-06-04.
- GUM (2008b) *Evaluation of measurement data – Supplement 1 to the "Guide to the expression of uncertainty in measurement" – Propagation of distributions using a Monte Carlo method*. JCGM 101:2008, <http://www.bipm.org/en/publications/guides/gum.html>, retrieved: 2015-06-04.
- Hennes M (2007) Konkurrierende Genauigkeitsmaße Potential und Schwächen aus der Sicht des Anwenders. *Allgemeine Vermessungs-Nachrichten*, **7**, 136–146.
- Hughes B, Forbes A, Lewis A, Sun W, Veal D, Nasr K (2011) Laser Tracker Error Determination Using a Network Measurement. In: *Meas. Sci. Technol.*, **22**, 1–12.
- Koch KR (1999) *Parameter Estimation and Hypothesis Testing in Linear Models*. Springer, Heidelberg/Berlin, 2nd edn.
- Lewis A, Hughes B, Forbes A, Sun W, Veal D, Nasr K (2011) Determination of misalignment and angular scale errors of a laser tracker using a new geometric model and a multi-target network approach. In: *Proceedings of the MacroScale 2011 – Recent developments in traceable dimensional measurements*, Federal Office of Metrology METAS, Wabern, Switzerland, DOI:10.7795/810.20130620S.
- Lösler M, Eschelbach C (2012) Concept of a Realisation of a Prototype for Adequate Evaluation of Polar Measurements (in German). *Allgemeine Vermessungs-Nachrichten*, **119**, 249–258.
- Lösler M, Haas R, Eschelbach C (2013) Automated and continual determination of radio telescope reference points with sub-mm accuracy: results from a campaign at the Onsala Space Observatory. *Journal of Geodesy*, **87**, 791–804, DOI:10.1007/s00190-013-0647-y.
- Lösler M, Eschelbach C, Haas R (2015) Zum Einfluss variierender Reflektorausrichtungen auf polare Messsysteme – Analytische Korrektur systematischer Zentrierabweichungen beim Messen auf bewegte Objekte. *GeoNews*, **3**, in-print.
- Mikhail EM, Ackerman F (1976) *Observations and Least Squares*, University Press of America, Lanham/Ney York/London.
- Muralikrishnan B, Sawyer DS, Blackburn CJ, Phillips SD, Borchardt BR, Estler WT (2009) ASME B89.4.19 Performance Evaluation Tests and Geometric Misalignments in Laser Trackers. In: *Journal of Research of the National Institute of Standards and Technology*, **114**, 21–35.
- Pauli W Vorteile eines kippbaren Reflektors bei der elektrooptischen Streckenmessung. *Vermessungstechnik*, 412–415, 1969.
- Rüeger JM *Electronic Distance Measurement - An Introduction*, Springer, Heidelberg/Berlin, 3rd edn., 1990.
- Schwarz W (1994) Zur Reduktion der Messungen bei räumlichen Punktbestimmungen. *Allgemeine Vermessungs-Nachrichten*, **101**, 207–218.
- Xu P (2013) The effect of incorrect weights on estimating the variance of unit weight. *Stud. Geophys. Geod.*, **57**, 339–352, DOI:10.1007/s11200-012-0665-x.